



This item was submitted to Loughborough's Institutional Repository (<https://dspace.lboro.ac.uk/>) by the author and is made available under the following Creative Commons Licence conditions.



CC creative commons
COMMONS DEED

Attribution-NonCommercial-NoDerivs 2.5

You are free:

- to copy, distribute, display, and perform the work

Under the following conditions:

 **Attribution.** You must attribute the work in the manner specified by the author or licensor.

 **Noncommercial.** You may not use this work for commercial purposes.

 **No Derivative Works.** You may not alter, transform, or build upon this work.

- For any reuse or distribution, you must make clear to others the license terms of this work.
- Any of these conditions can be waived if you get permission from the copyright holder.

Your fair use and other rights are in no way affected by the above.

This is a human-readable summary of the [Legal Code \(the full license\)](#).

[Disclaimer](#) 

For the full text of this licence, please go to:
<http://creativecommons.org/licenses/by-nc-nd/2.5/>

ELECTRICALLY ENHANCED REMOVAL OF SOLUTES FROM FILTER CAKES – INTERPRETATION OF PEAK MASS TRANSFER RATES

R.J. Wakeman¹, E.S. Tarleton¹ (e.s.tarleton@lboro.ac.uk), M.A. Koenders² and R. Kilchherr²

¹Advanced Separation Technologies Group, Dept. Chemical Engineering, Loughborough University, Loughborough, Leics., UK.

²Dept. Mathematics, Kingston University, Penrhyn Road, Kingston on Thames, Surrey, UK.

ABSTRACT

Some results from an experimental and theoretical investigation of cake washing assisted by d.c. electrical fields are reported. Electric fields are shown to increase the rate of removal of cations (Na^+) from rutile filter cakes when the downstream electrode was the cathode. For anions (NO_3^-) under the same experimental conditions, the removal rate also varied with the electric field but the effect was to slow the rate of mass transfer.

To give initial insight into the observed phenomena, the effects are explained through a first order model. The basic assumptions of the model are that: (1) there are two external forces driving the transport of ions: (i) a pressure difference that causes a mean fluid flow in which the ions are embedded, and (ii) the DC electric field applied across the cake; and (2) there are two pools of ions: (i) those trapped in the pores, and (ii) those that move with either the main fluid flow or the electrically generated ionic current.

The model demonstrates the same qualitative effects as seen in the experiments, with the magnitude of the effects dependent on the magnitudes of lateral and axial ion flux component constitutive forms.

INTRODUCTION

Filter cake washing assisted by electrical fields is a new area of technology that has received only limited attention by researchers¹⁻³. Although only slight increases in the kinetics of washing have been reported², the situation can be quite different when the removal of specific ions is measured³. In this paper an explanation is advanced for the peak mass transfer rates observed in washing experiments.

EXPERIMENTS

The downward filtering experimental apparatus used in this work is shown in Figure 1. The stainless steel rig comprised suspension and wash liquor feed reservoirs and a means for delivering compressed air to the filter at a controlled rate to maintain a constant pressure. Liquid from downstream of the filter test cell (area 120 cm²) was either directed to an electronic balance or, during washing, collected in sample bottles on a rotary table. A PC was used to record the mass of liquids discharged from the filter and the filtration/washing pressures and also to control the air pressure on the feed side of the filter cell. Iridium coated titanium mesh was chosen as a reasonably inert material for both the upper and lower electrodes. The lower electrode was just below the underside of a porous metal support on which a 0.2 μm rated Gelman Versapor filter medium rested. In all experiments the electrode spacing was maintained at 13 mm. A DC power supply was connected to the electrodes inside the filter and operated in the constant voltage mode.

An 8.6% v/v suspension of rutile (density 4260 kg m⁻³, mean particle size $\sim 0.3 \mu\text{m}$) in a solution of 0.001M or 0.01M NaNO_3 was prepared by adding a known amount of the dry powder to an aqueous NaNO_3 solution. The mixture was homogenised at 8000 rpm for 20 minutes. The pH of

Cite paper as: Wakeman R.J., Tarleton E.S., Koenders M.A. and Kilcherr R., 2003, Electrically enhanced removal of solutes from filter cakes – Interpretation of peak mass transfer rates, *Proc. Filtech Conference*, pp.249-256, Filtech Exhibitions, Dusseldorf, Germany. A version of this paper was also presented at the 9th World Filtration Congress, 2004, New Orleans, USA.

the feed suspension was adjusted with HNO₃ or NaOH. A stock salt solution was made by adding NaNO₃ into deionised (DI) water; the Na⁺ and NO₃⁻ were used as tracer ions to track the progress of the displacement washing. Zeta potentials were measured and the variation of zeta-potential with pH is shown in Figure 2. Measurements were carried out at two different ionic strengths over the pH range 3.5 to 9. For a 0.001M solution the IEP occurred at pH 5.2; for a 0.01M solution the IEP was at pH 5.8.

Prior to each experiment, all pipework was rinsed with DI water. Suspension at the required pH and ionic strength and DI water were added into the suspension vessel and washing liquid vessel respectively. A 10 mm thick filter cake was formed by constant pressure filtration in the absence of an electric field. Cake formation was followed by a displacement washing using DI water, either with or without the application of an electric field. In a typical sequence of experiments the applied voltage was varied over the range 0 to 30 V. During cake washing, both the hydraulic pressure and voltage remained constant and samples were collected and analysed for ion concentration. The cations were measured using atomic absorption spectroscopy and the anions using liquid chromatography. The moisture content and porosity of a filter cake were determined using gravimetric analysis either before or after the washing phase depending on the nature of an experiment.

RESULTS

The experiments were designed to observe the effects of the electric field, ionic strength, pH (zeta-potential) and electrode polarity on cake washing in terms of washing liquor flow rates and ion concentrations. The data are reported as washing curves, a plot of normalised instantaneous solute concentration (C/C_0) in the wash effluent versus wash time (t).

Figures 3 and 4 show how cation (Na⁺) and anion (NO₃⁻) concentrations in the wash liquor varied with wash time and applied voltage. In all cases the filtration pressure (Δp_f) and washing pressure (Δp_w) were 400 kPa and the initial suspensions were prepared in 10⁻³M NaNO₃ and adjusted to pH 7.8. For these conditions, the suspensions exhibited a zeta potential of -47 mV. During washing without an electric field, the instantaneous Na⁺ ion concentration in the wash liquors decreased in the initial period up to ~600 s and then reduced more rapidly with a tendency toward a limiting value. When an electric field was applied the normalised concentration of Na⁺ ions initially increased with time and reached the maximum values of 1.02 (at 10 V), 1.18 (at 20 V) and 1.24 (at 30 V), implying an accelerated removal of sodium ions from the cake with increasing electric voltage. A mass balance on the sodium ions washed from the cake suggested that some removal of Na⁺ ions from the particle surfaces may also have occurred; additional reslurry washing experiments without an electric field showed that there were Na⁺ ions on the particle surfaces that were removable by washing. In general, an electric field improved cake washing most effectively during the initial stages of washing and when the electric field strength was greater.

At longer washing times the Na⁺ concentration is higher when an electric field is applied than is the case when there is no applied potential. The implication from the 'tails' of the curves on Figure 3 is that there is a slow mechanism removing ions from the filter cake and that more ions are removed when an electric field is applied (this is reinforced when the area under the curves is calculated, showing more Na⁺ removal at higher applied voltages).

Regarding the NO₃⁻ anions, Figure 4 shows how the washing curve changed as the applied voltage was raised. The number of anions removed in the wash liquid decreased with an increasing electric field. When the downstream electrode is the cathode, the anions within the cake are subjected to an additional upward velocity. The direction of motion of the anions opposes both the electroosmotic flow and the flow induced by the hydraulic pressure gradient. The force causing counter-flow of the anions becomes more dominant as the applied voltage is increased.

A sequence of washing experiments with 10^{-2}M NaNO_3 ; all other conditions remained the same. Results showed the same general trends as those recorded in Figures 3 and 4. A slightly increased maximum dimensionless Na^+ concentration was noted when an electric field was applied (e.g. at 30 V, $(C/C_0)_{\text{max}}$ was 1.29 compared with 1.24 for the 10^{-3}M case). For a raised Na^+ ion concentration in the wash liquor there was generally a reduction in the NO_3^- ion concentration indicating a reduced washing performance with respect to anion removal.

Wash liquor flow rates were generally higher at 10^{-2}M NaNO_3 . The cake porosities were almost identical at each molar concentration, suggesting that there was an increased contribution from electroosmosis. As more salt is added to the initial suspension the double layer shrinks, tending to reduce the zeta potential of the rutile particles (Figure 2). At the higher ionic strength a larger current and power were consumed, particularly toward the beginning of washing where the ion concentration was at its highest (a maximum power $\sim 30\text{ W}$ was observed for $\Delta V = 30\text{ V}$). In the cases where an electric field was applied, the current decayed to a low value within a short period and this decay was more rapid at raised field strengths.

To assess the impact of zeta potential on electrowashing, filter cakes were also formed from suspensions close to their IEP (10^{-2}M NaNO_3 ; pH 5.2) and subsequently washed both with and without applied electric fields. Due to higher filter cake porosities it was necessary to reduce both filtration and washing pressures to 100 kPa to facilitate the experimental measurements. The results showed that both anions and cations behave in a generally similar manner to that noted for electrowashing at pH 7.8, although lower flow rates were recorded.

The variation of cake porosity with wash time was determined by performing two series of otherwise identical experiments where either no field was present or a 20 V potential was applied between the electrodes. Within each series, an experiment was stopped at a set time and cake samples taken to gravimetrically determine a porosity value corresponding to a given position on the wash curve. For the case of no electric field the largest change in cake porosity was noted during the first few minutes of washing after which there was essentially no further change. However, with an applied voltage of 20 V the average cake porosity was seen to fall from an initial value of 0.57 to a near constant value of 0.47 after a wash time of $\sim 1000\text{ s}$. At all times following the start of washing the cake porosity with no electric field exceeded that measured at an identical time with an applied field of 20 V.

THEORY

In a two-dimensional model the electric field is applied in the x -direction. Clean water is introduced at $x = 0$. The ion concentration measurement takes place at $x = L$ (next to the filter medium). There are two external forces that drive the transport of ions: (1) a pressure difference that causes a mean fluid flow in which the ions are embedded; (2) a DC electric field applied across the cake. The main driving force applied to the ions will be considered to be due to the electrical field. Strictly speaking, other phenomena such as electroosmotic mass flux contribute to ion migration, however the combination of the injection of DI water and slow fluid flow greatly reduce the contribution of that effect on ion mobility. The cake is formed by pressure filtration; colloids contributing to electrophoresis are therefore considered to be in small proportion. To strengthen these arguments, experimental data reveal that the potential difference between the electrodes situated at the extremities of the cake influence the ions velocity to a great extent.

Assume that there are two pools of ions: those trapped in the pores denoted by superscript (p) - and the ones that move with either the main fluid flow or the electrically generated ionic current, denoted by superscript (f). It is assumed that the (f) pool is subject to the electrical force such that they may move in the x -direction. The pool (p) may diffuse into the free flow; to do so they must acquire a y -direction motion.

The simplest model involves two species, positive and negative. So, there are four ion concentrations to be considered $C^{(1f)}$, $C^{(2f)}$, $C^{(1p)}$ and $C^{(2p)}$. These are functions of the position, x , and the time t . The velocities of the ions relative to the mean fluid velocity in the x -direction are $v^{(1f)}$, $v^{(2f)}$, $v^{(1p)}$, $v^{(2p)}$. These velocities may have two components and the species labelled (p) have a zero x -component. It is convenient to introduce the flux for each species of ion $J^{(i)}$. The equations of continuity take the following form

$$\frac{\partial C^{(1f)}}{\partial t} + \frac{\partial J_x^{(1)}}{\partial x} + \frac{J_y^{(1)}}{a} = 0 \quad (1)$$

$$\frac{\partial C^{(2f)}}{\partial t} + \frac{\partial J_x^{(2)}}{\partial x} + \frac{J_y^{(2)}}{a} = 0 \quad (2)$$

$$\frac{\partial C^{(1p)}}{\partial t} - \frac{J_y^{(1)}}{a} = 0 \quad (3)$$

$$\frac{\partial C^{(2p)}}{\partial t} - \frac{J_y^{(2)}}{a} = 0 \quad (4)$$

Where a is an internal length scale (of the order of magnitude of the mean particle radius), which is introduced for dimensional reasons. The rate of change of the pool of ions that is locked in the pores equals the influx; this influx must equal the outflux from the pool of freely moving particles at the same x -position. The latter may also change due to in and outflux in the flow direction.

Constitutive equations are now sought to characterise the physics of ionic migration. The velocity in the x -direction of the freely moving ions is ruled by the strength of the electric field, thus

$$J_x^{(1)} = A^{(1)} C^{(1f)} E \quad (5)$$

$$J_x^{(2)} = A^{(2)} C^{(2f)} E \quad (6)$$

Here the coefficients $A^{(*)}$ may be positive and negative, depending on the sign of the charge of the species. Their magnitude depends on the valence and process susceptibility. Essentially, $A^{(*)}E$ represents a velocity and the location of the peak in the output of some of the experiments corresponds to the time that the ions have travelled from one end to the other end of the filter. Calling this distance H and let the species of ion that displays the peak be the (1)-type, the time at which the peak occurs is

$$T_p = \frac{H}{A^{(1)}E} \quad (7)$$

Further constitutive refinements may be made to the transport velocity of the freely moving ions, especially diffusive effects should be added. These are proportional to $\partial C^{(fi)} / \partial x$; while they do not lead to non-linearity, such terms are most easily studied in a numerical context and in this first order exploration they are omitted.

A linear form for the constitutive form for the y -components of the flux is used here, suggesting that the efficacy with which ions are dislodged from the closed pores into the free flow regions is related to the concentration of the various species in the vicinity. Thus eight constitutive coefficients are introduced as follows

$$J_y^{(1)} = F^{(11)}C^{(1f)} + F^{(12)}C^{(2f)} + P^{(11)}C^{(1p)} + P^{(12)}C^{(2p)} \quad (8)$$

$$J_y^{(2)} = F^{(21)}C^{(1f)} + F^{(22)}C^{(2f)} + P^{(21)}C^{(1p)} + P^{(22)}C^{(2p)} \quad (9)$$

The coefficients encase the character of the process and may have various signs. The coefficients $P^{(11)}$ and $P^{(22)}$ are never zero: the outflux of ions from the pores must be proportional to the available concentration. Similarly, $F^{(11)}$ and $F^{(22)}$ are never zero: the influx of ions into the pores must be proportional to the available concentration in the free flowing pool. It is also easily verified that $P^{(11)}$ and $P^{(22)}$ are both negative and that $F^{(11)}$ and $F^{(22)}$ are both positive. They need not be exact opposites as the probability of an ion migrating into the pore is most likely not equal to the probability of one escaping from it. The role of the cross terms is also not immediately clear; it is likely that it is attractive for a positive ion to migrate from a pore into a region of plentiful negatives. On that basis the cross terms may have an influence and it is expected that $F^{(12)}$ and $F^{(21)}$ are both negative, while $P^{(12)}$ and $P^{(21)}$ are both positive. The cross terms may well be small when the solutions are dilute.

The linear form put forward here must be seen as a first order model; for not so dilute systems nonlinear effects will play a role. Again numerical simulation could shed more light on higher order effects; here the lowest order model is explored. The differential equations that rule the process are the following

$$\frac{\partial C^{(1f)}}{\partial t} + A^{(1)}E \frac{\partial C^{(1f)}}{\partial x} + \frac{F^{(11)}C^{(1f)} + F^{(12)}C^{(2f)} + P^{(11)}C^{(1p)} + P^{(12)}C^{(2p)}}{a} = 0 \quad (10)$$

$$\frac{\partial C^{(2f)}}{\partial t} + A^{(2)}E \frac{\partial C^{(2f)}}{\partial x} + \frac{F^{(21)}C^{(1f)} + F^{(22)}C^{(2f)} + P^{(21)}C^{(1p)} + P^{(22)}C^{(2p)}}{a} = 0 \quad (11)$$

$$\frac{\partial C^{(1p)}}{\partial t} - \frac{F^{(11)}C^{(1f)} + F^{(12)}C^{(2f)} + P^{(11)}C^{(1p)} + P^{(12)}C^{(2p)}}{a} = 0 \quad (12)$$

$$\frac{\partial C^{(2p)}}{\partial t} - \frac{F^{(21)}C^{(1f)} + F^{(22)}C^{(2f)} + P^{(21)}C^{(1p)} + P^{(22)}C^{(2p)}}{a} = 0 \quad (13)$$

The initial conditions are chosen to be constant in position and the same for all species and types:

$$C^{(1f)}(x,0) = C^{(2f)}(x,0) = C^{(1p)}(x,0) = C^{(2p)}(x,0) = C_0 \quad (14)$$

The boundary conditions states that fresh wash is flowed in at one end of the cake:

$$C^{(1f)}(0,t) = 0 \quad (15)$$

The entire cake must stay electrically neutral. Making use of the fact that the total charge vanishes and inserting the boundary condition at $x = 0$ results in

$$J_x^{(1)}(L) - J_x^{(2)}(L) + J_x^{(2)}(0) = 0 \quad (16)$$

The solution to the equations is obtained assuming that the cross terms $F^{(12)}$, $F^{(21)}$, $P^{(12)}$ and $P^{(21)}$ are negligible. A solution can be obtained using Laplace Transforms; although the general

analytical solution is difficult to obtain, the behaviour for small times is instructive. At the exit point of the flow $x = L$:

$$C^{(1f)}(L, t) = r_0 - \frac{r_0 (F^{(11)} + P^{(11)})}{a} t + \frac{r_0 (F^{(11)} + P^{(11)}) (F^{(11)} - P^{(11)})}{a^2} t^2 + \dots \quad (17)$$

The coefficient of the second term in the series in t is the derivative at $t = 0$. The output as a function of time increases when $F^{(11)} + P^{(11)} < 0$. It is recalled that $F^{(11)} > 0$ and $P^{(11)} < 0$. Behaviour that leads to a peak in the washing curve is therefore obtained when the probability of ions being released into the free flow from the pores is greater than vice versa.

To obtain information for the whole washing curve and not merely for short times, numerical analysis has been used. In Figure 5, the data for pH 7.8 is explored. The velocity is determined and should be of the form $v = v_0 + A^{(1)}E$ - since both the electric field and the pressure difference give the ions a velocity. Figure 5 shows reasonable agreement with this hypothesis.

The velocity is introduced as a phenomenological parameter and $P^{(11)}$ and $F^{(11)}$ are varied to give the best correspondence with the experimental outcome (again at pH 7.8); the calculated curves are shown in Figure 6. The theoretical effect that gives rise the presence or absence of the peak is recovered in the numerical approach.

In certain cases a curve such as C in Figure 6 displays a bending point. The location of this point may be obtained from the short-time approximation as

$$t_{bend} = \frac{a}{F^{(11)} - P^{(11)}} \quad (18)$$

Normally, the value that corresponds to this formula is in the order of 100's seconds, a further indication that the magnitude chosen for $P^{(11)}$ and $F^{(11)}$ is of the right order. This does not mean that $P^{(11)}$ and $F^{(11)}$ are independent of the applied field.

CONCLUSIONS

Electric fields increase the rate of removal of cations from rutile filter cakes when the downstream electrode is the cathode. For anions under the same experimental conditions, the removal rate slowed. A model demonstrates the same qualitative effects as seen in the experiments, with the magnitude of the effects dependent on the lateral and axial ion flux components.

REFERENCES

1. Larue O., Mouroko-Mitoulou T. and Vorobiev E., 2001, Filtration, cake washing and pressurised electroosmotic dewatering of a highly conductive silica suspension, *Trans. Filt. Soc.*, **1**(2), 31-37.
2. Ghirisan A., Weber K. and Stahl W., 2002, The influence of an electrical field on filtration and washing, *Trans. Filt. Soc.*, **2**(3), 56-60.
3. Tarleton E.S., Wakeman R.J. and Liang Y., 2003, Electrically enhanced washing of ionic species from fine particle filter cakes, *Trans IChemE*, **81**(A), 201-210.

TABLES AND FIGURES

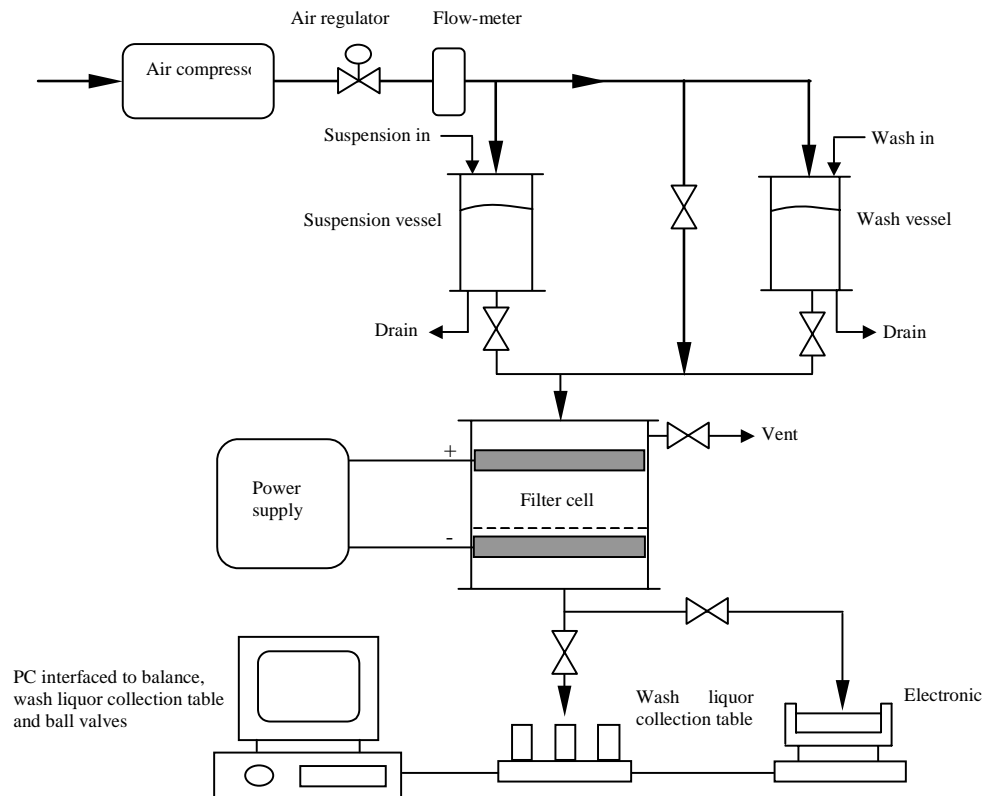


Figure 1: Schematic diagram of the experimental apparatus with the electrode polarity shown in the normal configuration.

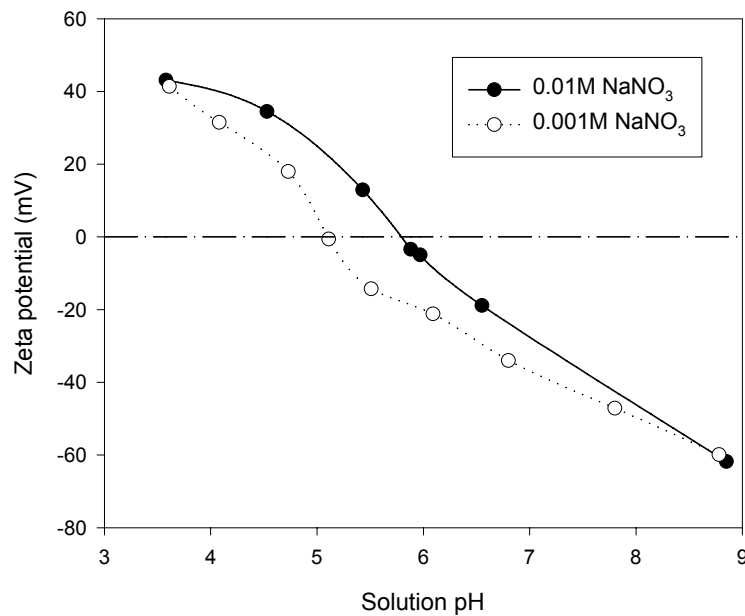
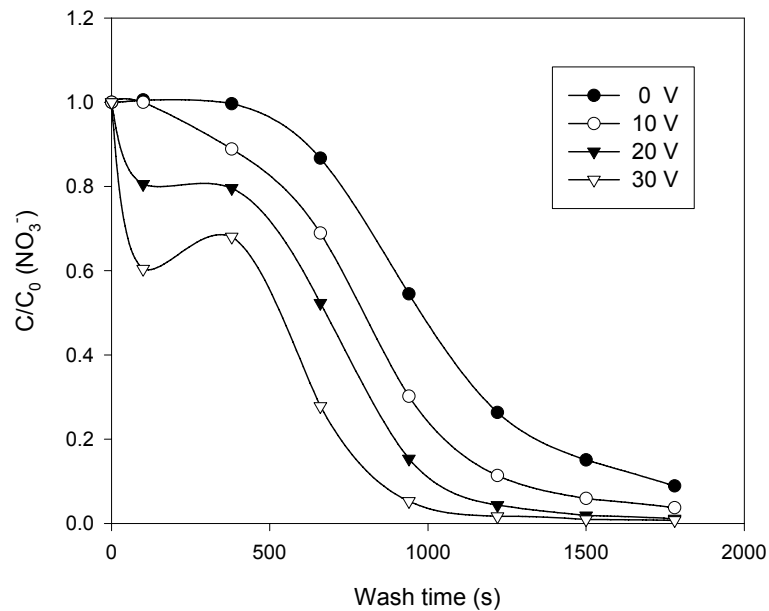
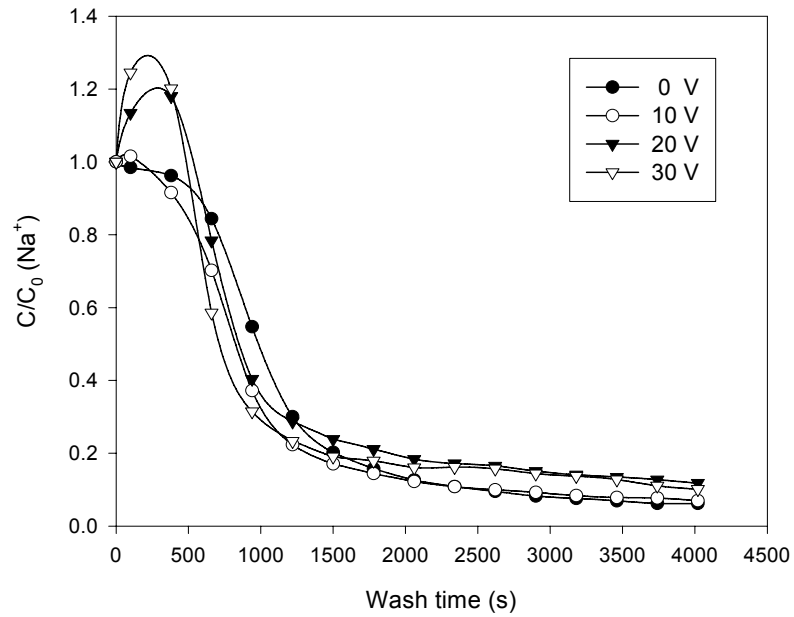


Figure 2: Zeta potential of rutile in aqueous solutions.



Figures 3 and 4: Variations of C/C_0 (Na^+) and C/C_0 (NO_3^-) in the wash liquor with time (t) and applied voltage ($\text{pH } 7.8$, 10^{-3} M NaNO_3 , $\Delta p_w = \Delta p_f = 400$ kPa).

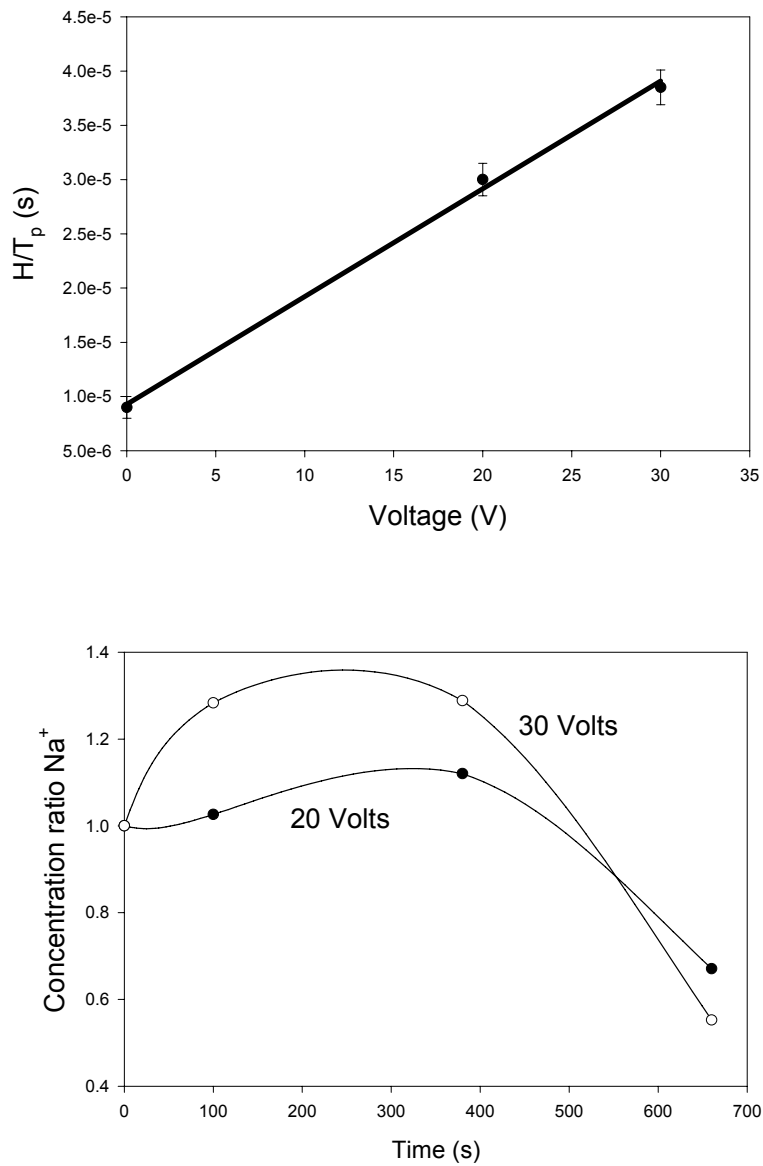


Figure 5: *Bottom*, location of the peak in the washing curve for pH 7.8; *Top*, location of the mean ion velocity as a function of the applied voltage.

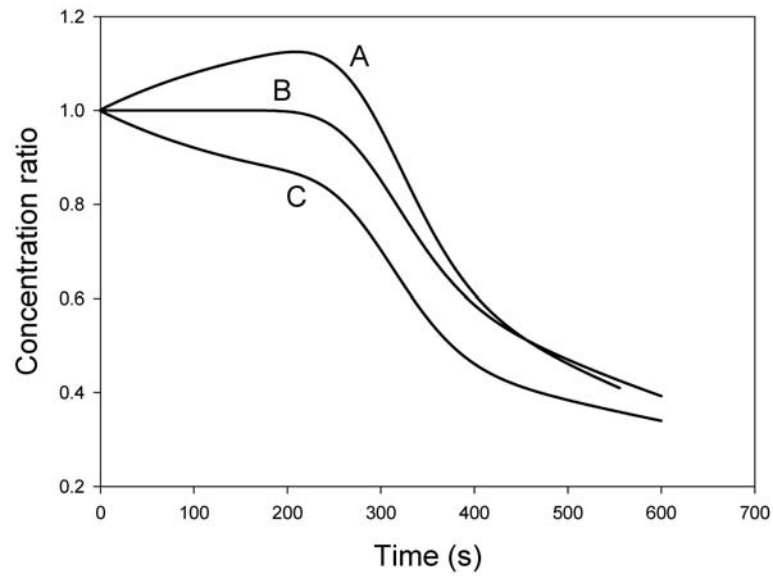


Figure 6: Concentration gradient as calculated by a numerical simulation for three sets of values for $P^{(11)}$ and $F^{(11)}$. A: $P^{(11)}/a = -.003 \text{ s}^{-1}$, $F^{(11)}/a = .002 \text{ s}^{-1}$; B: $P^{(11)}/a = -.003 \text{ s}^{-1}$, $F^{(11)}/a = .003 \text{ s}^{-1}$; C: $P^{(11)}/a = -.002 \text{ s}^{-1}$, $F^{(11)}/a = .003 \text{ s}^{-1}$.